Int. J. Electrochem. Sci., 7 **(2012)** 2047 - 2064

International Journal of
ELECTROCHEMICAL
SCIENCE
www.electrochemsci.org

Ionic Conductivity and Diffusion in Lithium Tetrafluoroborate-Doped 1-Methyl-3-Pentylimidazolium Tetrafluoroborate Ionic Liquid

Tzi-Yi Wu[1], *Lin Hao*[2], *Chung-Wen Kuo*[3], *Yuan-Chung Lin*[4], *Shyh-Gang Su*[2], *Ping-Lin Kuo*[5], *I-Wen Sun*[2,*]

[1] Department of Chemical Engineering and Materials Engineering, National Yunlin University of Science and Technology, Yunlin 64002, Taiwan, ROC
[2] Department of Chemistry, National Cheng Kung University, Tainan 70101, Taiwan
[3] Department of Chemical and Materials Engineering, National Kaohsiung University of Applied Sciences, Kaohsiung 80778, Taiwan
[4] Institute of Environmental Engineering, National Sun Yat-Sen University, Kaohsiung 804, Taiwan
[5] Department of Chemical Engineering, National Cheng Kung University, Tainan, 701, Taiwan, ROC
[*]E-mail: iwsun@mail.ncku.edu.tw

Received: 2 January 2012 / *Accepted:* 12 February 2012 / *Published:* 1 March 2012

Ion transport processes in mixtures of 1-methyl-3-pentylimidazolium tetrafluoroborate ([MPI][BF_4]) and lithium tetrafluoroborate ($LiBF_4$) are characterized using conductivity and pulsed field gradient NMR measurements at various temperatures. The viscosity, ionic conductivity, molar conductivity, and self diffusion coefficient in neat [MPI][BF_4] and $LiBF_4$-doped [MPI][BF_4] change with temperature following the Vogel-Tamman-Fulcher equation, and the density shows a linear decrease. The ionic conductivity and the self-diffusion coefficient of each ionic specie decrease with increasing concentration of $LiBF_4$ in $LiBF_4$-doped [MPI][BF_4]. The correlation between ionic conductivity and viscosity is based on the classical Walden rule, the α values of neat [MPI][BF_4] and $LiBF_4$-doped [MPI][BF_4] calculated from the slopes of the Walden plots are compared to those calculated from the ratio of activation energies for viscosity and molar conductivity ($E_{a,\Lambda}/E_{a,\eta}$). The comparison of activation energies of the reciprocal of viscosity, the ionic conductivity, and individual ion diffusion against the $LiBF_4$ concentration is also studied.

Keywords: Ionic liquid, ionic conductivity, molar conductivity, self-diffusion coefficient, ion transference number

1. INTRODUCTION

There is a rapidly expanding interest in using ionic liquids (ILs) as electrolyte materials for material science and electrochemical applications [1]. Ionic liquids (ILs), being defined as salts with

melting points below 100 ^{o}C, have attracted an enormous deal of attention because of their potential as green alternatives to common organic solvents [2]. Their intrinsic properties, like negligible volatility even at elevated temperature, nonflammability, high chemical and thermal stability, combined to high ionic conductivity [3-5] and electrochemical stability [6,7], make them very attractive candidates as electrolytes in rechargeable lithium batteries [8-11], electrochemical sensor [12-23], solar cells [24-28], fuel cell [29-31], and capacitors [32,33].

ILs are called "designer solvents" because their physicochemical properties can be easily tuned simply by changing the structures of the component cations and anions [34-36]. Currently, onium cation-based aprotic ILs such as quaternary ammonium and imidazolium RTILs have been adopted as "solvents" for use in Lithium ion batteries (LIBs)[37]. Most studies on ILs are dealing with imidazolium derivatives due to low viscosity and good ionic conductivity [38]. If intended to be used in Li batteries, ILs are required to have the ability to dissolve a Li salt to have a high Li^+ conductivity. Accordingly, the fundamental knowledge on physical and electrochemical properties of neat ILs and $LiBF_4$-doped ILs including viscosity, conductivity, and the diffusion coefficient is important [39-42]. Ion transport and diffusion in ionic liquids consisting of only one type of organic cation and one type of anion have been studied by means of ac impedance spectroscopy [43] and pulsed gradient spin-echo (PGSE) NMR techniques [44,45]. While the former technique provides information about the overall ionic conductivity, the latter technique is a method of choice for measuring self-diffusion of cations and anions, and its applications have grown exponentially in recent years ranging from probing the ionic diffusion coefficient, the degree of ionic association, and the interaction between ions [46]. The importance and dominance of this technique lies in it being able to provide the diffusion coefficient (D) of multiple species in a sample simultaneously and in a noninvasive manner.

In this work, we report the effects of ionic conductivity, viscosity, and ion self-diffusion coefficients for a mixture of 1-methyl-3-pentylimidazolium tetrafluoroborate ([MPI][BF_4]) and $LiBF_4$. To evaluate the possibility of using binary [MPI][BF_4] and $LiBF_4$ electrolytes, the solubility of lithium salt in [MPI][BF_4] is examined, homogeneous binary ILs were obtainable over a wide range of salt concentrations. For instance, the molar ratio of $x_{LiBF_4} = 0.25$ is obtainable at room temperature without crystallization. The relationship between the ionic conductivity and the viscosity in the neat [PMI][BF_4] and $LiBF_4$-doped [MPI][BF_4] is analyzed using the Walden rule. The self-diffusion coefficients of the ionic species holding ^{1}H, ^{7}Li, or ^{19}F nuclei are measured as a function of the $LiBF_4$ mole fraction x by using the pulsed gradient spin-echo NMR (PGSE-NMR) method to bring some information on the transport properties of the various ionic species.

2. EXPERIMENTAL

2.1. Materials and measurement

1-Methylimidazole (99%), 1-bromopentane (99%), sodium tetrafluoroborate (99%), and lithium tetrafluoroborate (99%) were obtained from Aldrich, TCI, and Acros and used as received. The conductivity (σ) of the ionic liquid was systematically measured with a conductivity meter LF 340 and

a standard conductivity cell TetraCon 325 (Wissenschaftlich-Technische Werkstätten GmbH, Germany). The cell constant was determined by calibration after each sample measurement using an aqueous 0.01 M KCl solution. The density of the ILs was measured with a dilatometer, which was calibrated by measuring the density of deionized water at 20, 30, 40 and 50 ^{o}C. To measure the density, IL or binary mixture was placed into the dilatometer up to the marks, sealed the top of capillary tube, which was on the top of the dilatometer, and placed into a temperature bath for 10 minutes to allow the temperature to equilibrate. The main interval between two marks in capillary tube is 0.1 cm^3, and the minor interval between two marks is 0.01 cm^3. From the correction coefficient of deionized water in capillary tube at various temperatures, we can calculate the density of neat IL or binary system by the expanded volume of liquid in capillary tube at various temperatures. Each sample was measured at least three times to determine an average value, and the values of the density are ± 0.0001 g mL^{-1}. The viscosities (η) of the ILs were measured using a calibrated modified Ostwald viscometer (Cannon-Fenske glass capillary viscometers, CFRU, 9721-A50) with inner diameters of 1.2 ± 2% mm. The viscometer was placed in a thermostatic water bath (TV-4000, TAMSON), in which the temperature was regulated to within ± 0.01 K. The flow time was measured with a stop watch capable of recording to 0.01 s. For each IL, the experimental viscosity was obtained by averaging three to five flow time measurements. The water content of the dried ILs was detected by a Karl–Fischer moisture titrator (Metrohm 73KF coulometer), and the values were less than 150 ppm. NMR spectra of synthetized ILs were recorded on a BRUKER AV300 spectrometer and calibrated with tetramethylsilane (TMS) as the internal reference.

2.2. Synthesis of 1-methyl-3-pentylimidazolium tetrafluoroborate [MPI][BF_4]

1-bromopentane (208 g, 1.38 mol) was added to a vigorously stirred solution of 1-methylimidazole (102.6 g, 1.25 mol) in toluene (125 mL) at 0 ^{o}C. The solution was heated to reflux at around 110 ^{o}C for 24 hours, and then cooled to room temperature for 12 hours. The toluene was decanted and the remaining viscous oil was washed with ether several times to yield a viscous liquid, which was dried *in vacuo* to give 1-pentyl-3-methylimidazolium bromide ([MPI][Br]) with a yield of approximately 82 %. ^{1}H-NMR (400MHz, D_2O, ppm): δ 0.80 (t, J = 7.1 Hz, 3H, CH_3), δ 1.14-1.33 (m, 4H, CH_2), δ 1.76-1.86 (m, 2H, CH_2), δ 3.84 (s, 3H, CH_3), δ 4.14 (t, J = 7.1 Hz, 2H, CH_2), δ 7.37-7.40 (m, 1H, CH), δ 7.42-7.44 (m, 1H, CH), δ 8.67 (s, 1H, CH). ^{13}C-NMR (100 MHz, D_2O, ppm): 13.5 (q), 21.6 (t), 27.7 (t), 29.2 (t), 36.1 (q), 49.7 (t), 122.4 (d), 123.7 (d), 135.9 (d). Elemental analysis (%) is found (C, 46.26; H, 7.32; N, 11.97) and calculated (C, 46.36; H, 7.35; N, 12.02) for synthetic [MPI][Br]. $NaBF_4$ (0.32 mol) was added to a solution of [MPI][Br] (0.29 mol) in dichloromethane and stirred for 24 hours. The suspension was filtered to remove the precipitated bromide salt. The organic phase was repeatedly washed with small volumes of water (around 30 cm^3) until no precipitation of AgBr occurred in the aqueous phase upon the addition of a concentrated $AgNO_3$ solution. The organic phase was then washed two more times with water to ensure the complete removal of the bromide salt. The solvent was removed *in vacuo* and the resulting IL was stirred with activated charcoal for 12 hours. The IL was then passed through a short alumina column(s) (acidic and/or neutral) to give a

colorless IL, which was dried at 100 ^{o}C *in vacuo* for 24 hours or until no visible signs of water were present in the IR spectrum. Yields were 70 to 80 %. ^{1}H-NMR (400MHz, D_2O, ppm): δ 0.76-0.84 (m, 3H, CH_3), δ 1.14-1.33 (m, 4H, CH_2), δ 1.74-1.86 (m, 2H, CH_2), δ 3.79-3.86 (m, 3H, CH_3), δ 4.08-4.17 (m, 2H, CH_2), δ 7.33-7.43 (m, 2H, CH), δ 8.60 (s, 1H, CH). ^{13}C-NMR (100MHz, D_2O, ppm): 13.1 (q), 21.6 (t), 27.7 (t), 29.2 (t), 35.5 (q), 49.4 (t), 122.2 (d), 123.5 (d), 136.1 (d). Elemental analysis (%) is found (C, 45.12; H, 7.11; N, 11.53) and calculated (C, 45.03; H, 7.14; N, 11.67) for synthetic [MPI][BF_4]. The Br^- contents were confirmed with ICP-MS, being below 0.5% w/w. The structure of 1-methyl-3-pentylimidazolium tetrafluoroborate is shown in Fig. 1.

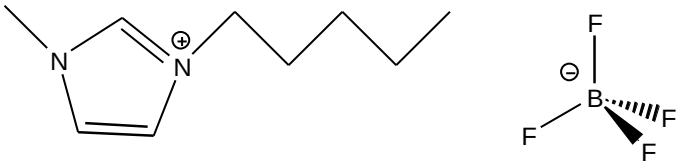

Figure 1. Chemical structure of 1-methyl-3-pentyl-imidazolium tetrafluoroborate ([MPI][BF_4]).

2.3. Sample preparation for diffusion coefficient measurements

A portion of each sample was degassed and sealed in a cylindrical Pyrex tube under high vacuum at room temperature. The sealed sample tube was inserted into a standard 5 mm tube filled with an external lock solvent of D_2O. ^{1}H, ^{19}F, ^{7}Li NMR measurements were carried out on a Bruker Avance 400 with a 5 mm pulsed-field gradient probe. The signals of ^{1}H in $[MPI]^+$, ^{7}Li in Li^+, and ^{19}F in tetrafluoroborate anions were used for the determination of self-diffusion coefficients (D_{MPI^+}, D_{Li^+}, and $D_{BF_4^-}$) of the cation and anion species, respectively. The sample temperature was controlled within ±0.1K by a variable temperature control unit using heated.

Pulsed-gradient spin-echo diffusion measurements were carried out using a stimulated spin-echo sequence. In the pulsed-field gradient spin-echo NMR experiment, the self-diffusion coefficient, *D*, is given by Tanner and Stejskal [47]:

$$\ln\left(\frac{A}{A_0}\right) = -D\gamma^2(\Delta - \frac{\delta}{3})\delta^2 g^2 \qquad (1)$$

where *A* and A_0 are the signal integrals in the presence and absence of the pulsed-field gradient, respectively, γ is the nuclear magnetogyric ratio, Δ is the interval between the two gradient pulses, δ is the gradient pulse width, and *g* is the gradient magnitude. In the present experiments, the pulse-field-gradient interval Δ determines the diffusion time and was varied from 20 to 100 ms, δ was set between 3 and 18 ms, and *g* was set using a suitable strength. The self-diffusion coefficients were measured five or more times at each temperature. The experimental errors in D_{MPI^+}, D_{Li^+}, and $D_{BF_4^-}$ were estimated to be less than 3%.

3. RESULTS AND DISCUSSION

3.1. Ionic conductivity and viscosity of neat [MPI][BF$_4$] and LiBF$_4$-doped [MPI][BF$_4$]

The fundamental properties of neat [MPI][BF$_4$] and LiBF$_4$-doped [MPI][BF$_4$], including physicochemical quantities of density (ρ), viscosity (η), and conductivity (σ), are plotted in Fig. 2-4, all of the LiBF$_4$-doped [MPI][BF$_4$] are liquid at room temperature.

Generally, in a narrow range of temperatures, ρ (g cm^{-3}) can be expressed as follows:

$$\rho = A + BT \qquad (2)$$

where A, B, and T are the density at 0 K (g cm^{-3}), the coefficient of volume expansion (g cm^{-3} K^{-1}), and temperature (K), respectively. In the present system a strong linear relationship ($R > 0.999$) with temperature was obtained for neat [MPI][BF$_4$] and LiBF$_4$-doped [MPI][BF$_4$] (Fig. 2). The best fit parameters of Eq. (2) are summarized in Table 1. As shown in Fig. 2, the density of lithium tetrafluoroborate-doped RTIL increases with increasing lithium tetrafluoroborate concentration, for instance, LiBF$_4$-doped RTIL (x_{LiBF_4} = 0.0672, ρ = 1.1960 g cm^{-1} at 30 ^{o}C) has higher density than IL without doping LiBF$_4$ (ρ = 1.1746 g cm^{-1} at 30 ^{o}C), x_{LiBF_4} = 0.1543 (ρ = 1.2164 g cm^{-1} at 30 ^{o}C) has higher density than x_{LiBF_4} = 0.1111 (ρ = 1.2063 g cm^{-1} at 30 ^{o}C). In lithium tetrafluoroborate-doped RTIL, a more efficient packing and/or attractive interaction occurred when the ionic liquid and LiBF$_4$ were mixed, small lithium ion fit into the interstices upon mixing. Therefore, the filling effect of lithium ion in the interstices of ionic liquids contributes to a denser structure.

Table 1. The adjustable parameters of density ($\rho = A + B \cdot T$) for neat [MPI][BF$_4$] and LiBF$_4$-doped [MPI][BF$_4$] at various LiBF$_4$ concentrations.

Mole fraction of LiBF$_4$	ρ		
	A	10^4B	R^{2a}
neat [MPI][BF$_4$]	1.369	–6.413	0.9999
x_{LiBF_4} = 0.0672	1.391	–6.433	0.9998
x_{LiBF_4} = 0.1111	1.403	–6.488	0.9996
x_{LiBF_4} = 0.1543	1.414	–6.517	0.9997
x_{LiBF_4} = 0.2054	1.419	–6.486	0.9999
x_{LiBF_4} = 0.2503	1.441	–6.561	0.9998

[a] Correlation coefficient.

The viscosity of an IL is related to the ability of its constituting particles to move in response to an applied force and the conductivity refers to the mobility of the ions. The relative viscosity (Li-salt-doped sample/neat RTIL sample) is depicted in Fig. 3. The viscosity values, η, were fitted using Vogel–Tamman–Fulcher (VTF) equation and modified Vogel–Tamman–Fulcher (modified VTF)

equation. The most commonly used equation to correlate the variation of viscosity with temperature is the Arrhenius-like law, but according to Seddon et al. [48] the Arrhenius law can generally be applied when the cation presents only a limited symmetry.

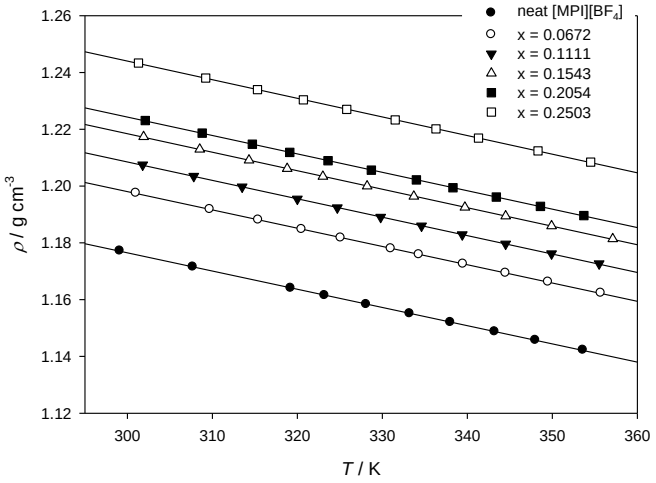

Figure 2. Temperature dependence of density data for neat [MPI][BF_4] and $LiBF_4$-doped [MPI][BF_4].

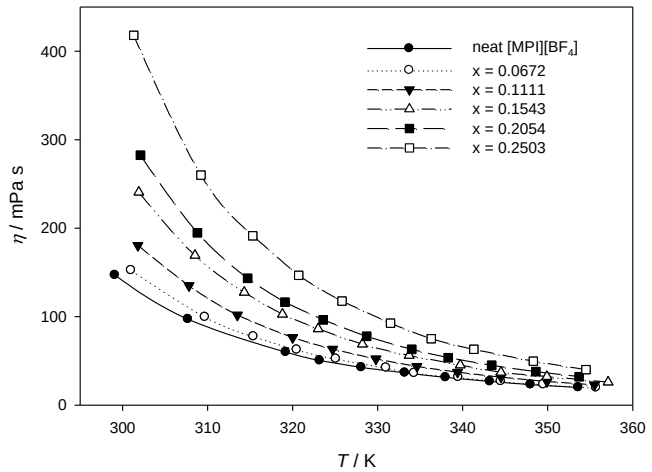

Figure 3. Dynamic viscosity (η) as a function of temperature for neat [MPI][BF_4] and $LiBF_4$-doped [MPI][BF_4].

If this is not the case, Vogel–Tamman–Fulcher (VTF) and modified equation Vogel–Tamman–Fulcher are recommended [48]. The modified VTF equation can be expressed as:

$$\eta^{-1} = \frac{\eta_o}{\sqrt{T}} \exp[\frac{-B}{(T - T_o)}] \qquad (3)$$

and the VTF equation can be presented as:

$$\eta^{-1} = \eta_o \exp[\frac{-B}{(T - T_o)}] \quad (4)$$

where η_o, B, and T_o are adjustable parameters. The best-fit η_o (mPa s), B (K), and T_o (K) parameters are given in Table 2. The viscosity of neat [MPI][BF_4] and $LiBF_4$-doped [MPI][BF_4] follows the order: neat [MPI][BF_4] < (x_{LiBF_4} = 0.0672) < (x_{LiBF_4} = 0.1111) < (x_{LiBF_4} = 0.1543) < (x_{LiBF_4} = 0.2054) < (x_{LiBF_4} = 0.2503). The addition of a Li salt to [MPI][BF_4] increased viscosity due to the enhancement of ion-ion interactions.

Table 2. The VTF equation parameters of viscosity ($\eta = \eta_o \exp[B/(T - T_o)]$) and conductivity ($\sigma = \sigma_o \exp[-B'/(T - T_o)]$).

Mole fraction of $LiBF_4$	η				σ			
	η_o / mPa s	T_o / K	B / K	R^{2a}	σ_o / mS cm^{-1}	T_o / K	B' /K	R^{2a}
neat [MPI][BF_4]	0.182	170.5	860.9	0.999	87.6	194.0	381.9	0.999
x_{LiBF_4} = 0.0672	0.173	173.4	865.0	0.999	52.0	208.4	295.4	0.999
x_{LiBF_4} = 0.1111	0.156	171.3	920.6	0.999	59.9	204.0	339.3	0.999
x_{LiBF_4} = 0.1543	0.135	170.6	983.3	0.999	102.6	184.2	500.6	0.999
x_{LiBF_4} = 0.2054	0.193	179.1	896.7	0.999	78.9	191.3	452.0	0.999
x_{LiBF_4} = 0.2503	0.192	178.5	943.9	0.999	80.8	191.7	482.7	0.999

[a] Correlation coefficient.

Table 3. The E_a, ΔS and ΔH evaluated by Eyring equation and the relationships of η vs. T and σ vs. T.

Mole fraction of $LiBF_4$	η			σ		
	E_a/ kJ $mole^{-1}$	ΔS/ J $mole^{-1}$ K^{-1}	ΔH/ kJ $mole^{-1}$	E_a/ kJ $mole^{-1}$	ΔS/ J $mole^{-1}$ K^{-1}	ΔH/ kJ $mole^{-1}$
neat [MPI][BF_4]	31.95	-319.80	34.66	21.63	-174.21	19.01
x_{LiBF_4} = 0.0672	33.21	-323.05	35.93	18.97	-184.20	16.24
x_{LiBF_4} = 0.1111	34.35	-325.03	37.07	20.21	-181.40	17.49
x_{LiBF_4} = 0.1543	36.17	-328.75	38.90	22.10	-177.31	19.38
x_{LiBF_4} = 0.2054	37.08	-330.35	39.80	22.30	-177.40	19.59
x_{LiBF_4} = 0.2503	38.76	-333.08	41.48	23.68	-175.07	20.95

For the relationship of η vs. T, the E_a, ΔS, and ΔH values evaluated using the slope ($-E_a/R$) of the Arrhenius equation and Eyring equation for the ILs are summarized in Table 3. The absolute values of E_a, ΔS, and ΔH for the ILs are in the order: (1) $LiBF_4$-doped [MPI][BF_4], x_{LiBF_4} = 0.0672 (E_a = 33.21 kJ $mole^{-1}$, $|\Delta S|$ = 323.05 J $mole^{-1}$ K^{-1}, and ΔH = 35.93 kJ $mole^{-1}$) > [MPI][BF_4] without doping $LiBF_4$ (E_a = 31.95 kJ $mole^{-1}$, $|\Delta S|$ = 319.80 J $mole^{-1}$ K^{-1}, and ΔH = 34.66 kJ $mole^{-1}$); (2) higher mole fraction

of $LiBF_4$ (x_{LiBF_4} : 0.2054, E_a = 37.08 kJ mole^{-1}, $|\Delta S|$ = 330.35 J mole^{-1} K^{-1}, and ΔH = 39.80 kJ mole^{-1}) > lower mole fraction of $LiBF_4$ (x_{LiBF_4} : 0.1543, E_a = 36.17 kJ mole^{-1}, $|\Delta S|$ = 328.75 J mole^{-1} K^{-1}, and ΔH = 38.90 kJ mole^{-1}).

Ionic conductivity was measured for different molar ratios of the [MPI][BF_4]–$LiBF_4$ electrolytes at various temperatures. The conductivity (σ) is related to the ion mobility and the number of charge carriers, which can be expressed by the following equation [49,50]:

$$\sigma = \sum n_i q_i u_i \qquad (5)$$

where n_i, q_i, and u_i are the number of charge carriers of type i, the charge of each species, and the mobility of each species, respectively. The temperature dependence of conductivity for these ILs is depicted in Fig. 4. An increase in temperature results in an increase in the mobility because the viscosity of the liquids is reduced. The observed temperature dependences of conductivity are well fitted by VTF equation:

$$\sigma = \sigma_o \exp[\frac{-B'}{(T - T_o)}] \qquad (6)$$

where σ_o, B', and T_o were the fitting parameters. The VTF fitting parameters of the ionic conductivity for these ILs are summarized in Table 2.

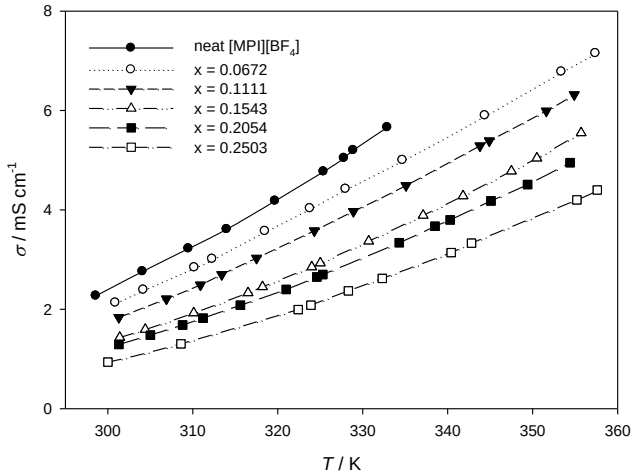

Figure 4. Dependence of specific conductivity (σ) on temperature for neat [MPI][BF_4] and $LiBF_4$-doped [MPI][BF_4].

Different from viscosity, the conductivity of ILs decreases initially upon addition of $LiBF_4$, and then increases with increasing x_{LiBF_4} following the order: neat [MPI][BF_4] > (x_{LiBF_4} = 0.0672) > (x_{LiBF_4} = 0.1111) > (x_{LiBF_4} = 0.1543) > (x_{LiBF_4} = 0.2054) > (x_{LiBF_4} = 0.2503). For the relationship of σ vs. T, the E_a, ΔS, and ΔH values evaluated using the slope (-E_a/R) of the Arrhenius and Eyring equations for the ILs

are summarized in Table 3. E_a, ΔS, and ΔH decrease initially upon addition of $LiBF_4$, and then increases with further addition of $LiBF_4$ ($x_{LiBF_4} \geq 0.1111$).

Ionic conductivity is proportional to the concentration of free ions and the mobility of the ions. The molar conductivity Λ (S cm^2 mol^{-1}) was obtained by dividing the ionic conductivity by the salt concentration according to the following equation:

$$\Lambda = \sigma \frac{M}{\rho} \quad (7)$$

where M, σ, ρ are the respective equivalent weight, specific conductivity, and density of the IL mixtures. The temperature dependence of molar conductivity for the IL mixtures is depicted in Figure 5. The observed temperature dependences of molar conductivity are well fitted by the empirical VTF equation:

$$\Lambda = \Lambda_o \exp[\frac{-B'}{(T - T_o)}] \quad (8)$$

where Λ_o, B', and T_o are the fitting parameters. VTF fitting parameters of the molar conductivity for the ILs are summarized in Table 4. With regard to the relationship of Λ vs. T, the E_a, ΔS, and ΔH values evaluated using the slope ($-E_a$/R) of the Arrhenius and Eyring equations for the ILs are summarized in Table 5. The E_a, ΔS, and ΔH values of the molar conductivity (Λ) show similar tendency with specific conductivity (σ).

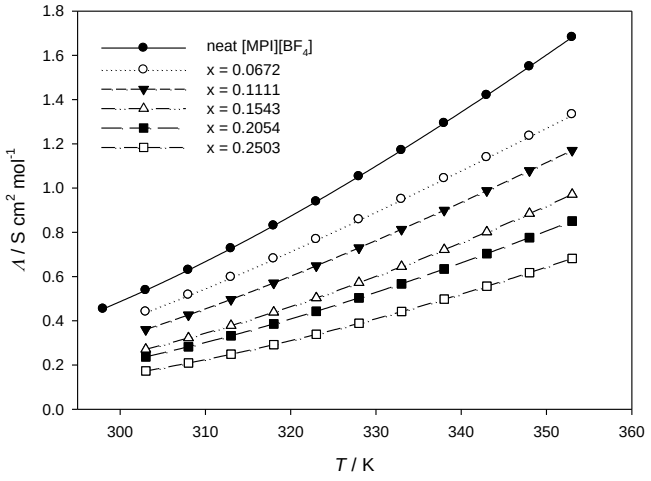

Figure 5. Dependence of molar conductivity (Λ) on temperature for neat [MPI][BF_4] and $LiBF_4$-doped [MPI][BF_4].

Table 4. VTF equation parameters of molar conductivity data ($\Lambda = \Lambda_o \exp[-B'/(T - T_o)]$, $\Lambda_{NMR} = \Lambda_o \exp[-B'/(T - T_o)]$)

Molar fraction of $LiBF_4$	Λ				Λ_{NMR}			
	Λ_o / S cm^2 mol^{-1}	T_o/K	B'/K	R^{2a}	Λ_o / S cm^2 mol^{-1}	T_o /K	B' /K	R^{2a}
neat [MPI][BF_4]	23.2	187.9	433.0	0.999	218.3	201.6	540.9	0.999
x_{LiBF_4} = 0.0672	11.5	205.8	316.9	0.999	226.6	199.4	595.1	0.999
x_{LiBF_4} = 0.1111	12.8	201.4	362.4	0.999	364.6	186.7	758.8	0.999
x_{LiBF_4} = 0.1543	21.6	181.4	531.8	0.999	330.3	190.6	738.4	0.999
x_{LiBF_4} = 0.2054	15.8	188.7	479.8	0.999	280.6	193.2	740.6	0.999
x_{LiBF_4} = 0.2503	15.4	189.3	510.1	0.999	437.3	182.2	904.2	0.999

[a] Correlation coefficient.

Recently, it has been reported that the Walden rule is roughly applicable in ILs, and is a useful measure for examination of the ion pairing problem in electrolyte solution. If the viscosity and conductivity of the electrolyte obeys Walden's rule, the ionic conductivity is correlated to viscosity using the qualitative approach of Angell et al. [51]:

$$\Lambda \eta^{\alpha} = C \qquad (9)$$

where C is a temperature-dependent constant, which is called the Walden product. α is the slope of the line in the Walden plot, which reflects the decoupling of the ions. The fitted α values of the ILs are given in Table 6. The parameter α reflects the difference of the activation energies of the ionic conductivity and viscosity. In the present study, all α values are smaller than unity (α < 1), indicating that the ionic conductivities of the liquid salts is somewhat diminished as a result of ion-pair formation [1].

Moreover, combining the data from viscosity, conductivity and density measurements we find the molar conductivities of ILs with x_{LiBF_4} = 0, 0.0672, 0.1111, 0.1543, 0.2054, and 0.2503 to be 0.538, 0.441, 0.361, 0.271, 0.237, and 0.173 S cm^2 mol^{-1} at 30 ^{o}C, respectively. Another method that yields almost identical values of α is the ratio of the temperature-dependent activation energies for viscosity and molar conductivity, $E_{a,\Lambda}/E_{a,\eta}$ [52]. The activation energies of $E_{a,\Lambda}$ and $E_{a,\eta}$ are summarized in Table 3 and Table 5.

Table 6 compares α values calculated from the slopes of the Walden plots in Fig. 6 with those calculated from the activation energies. The two methods for obtaining α values are in very good agreement.

Table 5. The E_a, ΔS and ΔH evaluated by Eyring equation and the relationships of Λ vs. T and Λ_{NMR} vs. T.

Molar fraction of $LiBF_4$	Λ			Λ_{NMR}		
	E_a/ kJ mole^{-1}	ΔS/ J mole^{-1} K^{-1}	ΔH/ kJ mole^{-1}	E_a/ kJ mole^{-1}	ΔS/ J mole^{-1} K^{-1}	ΔH/ kJ mole^{-1}
neat [MPI][BF_4]	20.70	-190.62	18.01	31.11	-150.29	28.39
x_{LiBF_4} = 0.0672	19.54	-195.94	16.82	33.00	-147.12	30.28
x_{LiBF_4} = 0.1111	20.79	-193.46	18.08	34.51	-144.70	31.79
x_{LiBF_4} = 0.1543	22.58	-190.00	19.86	35.48	-142.62	32.77
x_{LiBF_4} = 0.2054	22.61	-190.38	19.89	37.25	-139.65	34.53
x_{LiBF_4} = 0.2503	24.25	-188.15	21.54	38.69	-137.41	35.97

Table 6. Comparison of the activation energies for the absolute viscosity, $E_{a,\eta}$, and equivalent conductance, $E_{a,\Lambda}$. α is from the general Walden plots and α_{EA} is calculated from the ratio of the activation energies ($E_{a,\Lambda}$ / $E_{a,\eta}$).

Molar fraction of $LiBF_4$	$E_{a,\eta}$ / kJ mole^{-1}	$E_{a,\Lambda}$ / kJ mole^{-1}	α	α_{EA}
neat [MPI][BF_4]	32.0	20.7	0.639	0.648
x_{LiBF_4} = 0.0672	33.2	19.5	0.586	0.588
x_{LiBF_4} = 0.1111	34.4	20.8	0.602	0.605
x_{LiBF_4} = 0.1543	36.2	22.6	0.620	0.624
x_{LiBF_4} = 0.2054	37.1	22.6	0.611	0.610
x_{LiBF_4} = 0.2503	38.8	24.3	0.631	0.626

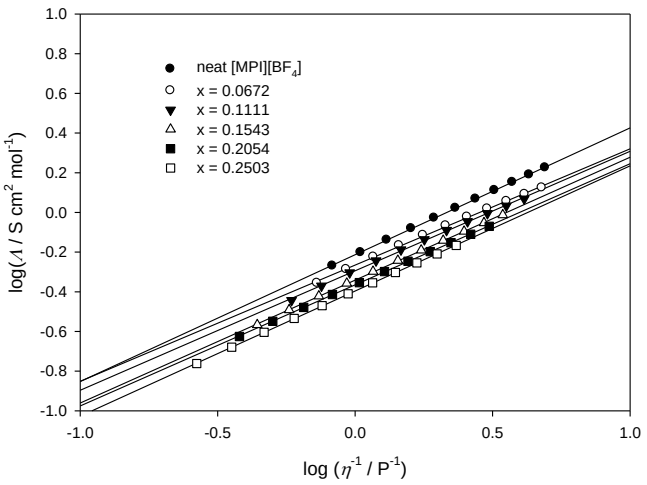

Figure 6. Walden plots for neat [MPI][BF_4] and $LiBF_4$-doped [MPI][BF_4], where Λ is the equivalent conductivity and η^{-1} is the fluidity. The solid lines are the result of linear regressions onto the data.

According to the Walden rule, ILs that possess strongly interacting ions in ILs are usually located below the KCl ideal line, due to partial association of neighboring ions. In the present study, $LiBF_4$-doped [MPI][BF_4] and neat [MPI][BF_4] are less than the $\Lambda\eta$ of the KCl aqueous solution, indicating a fraction of ion association in the ILs. Compare the discrepancy from the ideal line of Walden plots, the deviation increases significantly with the addition of $LiBF_4$ to [MPI][BF_4], implying the addition of $LiBF_4$ increases the ion association in the IL mixture.

3.2. Self-Diffusion Coefficient of the Individual ion

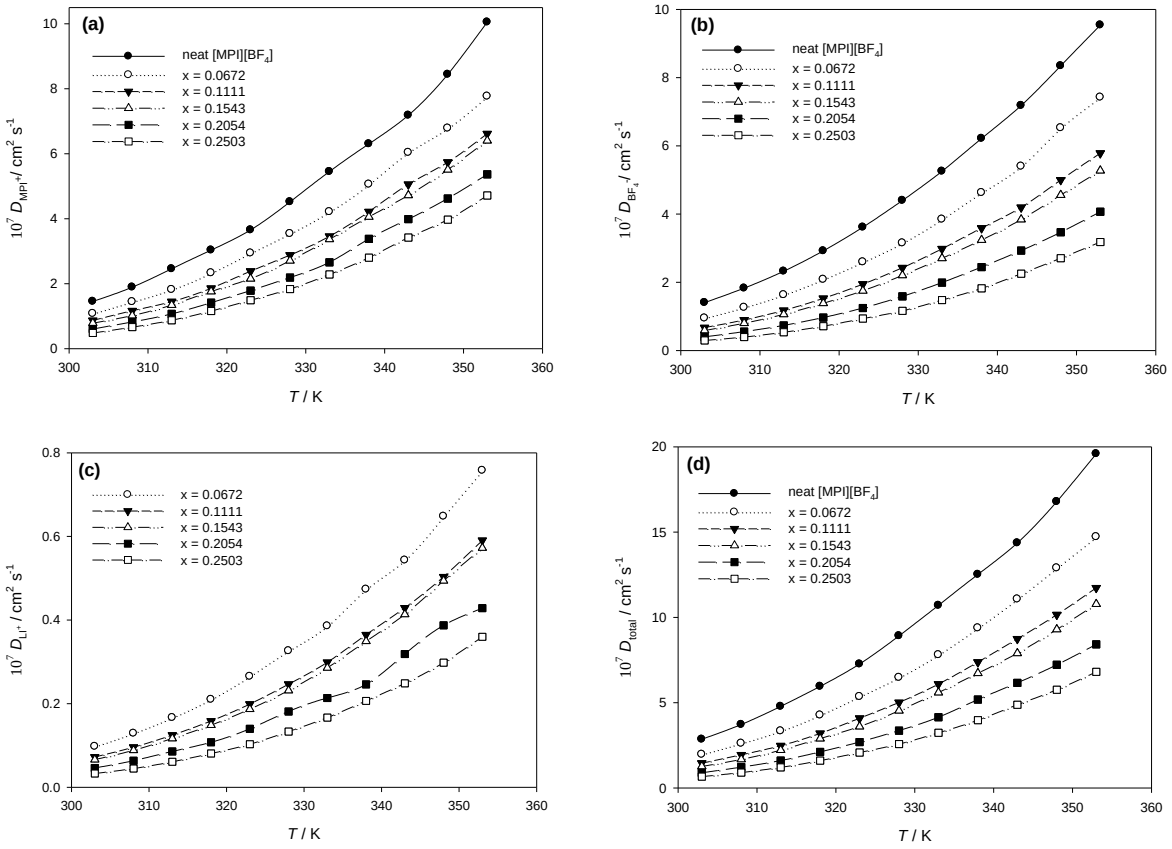

Figure 7. Temperature dependence of the self-diffusion coefficients of ions (a) D_{MPI^+}, (b) $D_{\mathrm{BF_4}^-}$, (c) D_{Li^+}, and (d) D_{total} in neat [MPI][BF_4] and $LiBF_4$-doped [MPI][BF_4].

Pulsed-field gradient spin-echo (PGSE) NMR measurements were carried out to determine the self-diffusion coefficients of individual ion in neat [MPI][BF_4] and $LiBF_4$-doped [MPI][BF_4]. The diffusion coefficients of the ^1H, ^7Li, and ^{19}F nuclei have been measured as a function of the $LiBF_4$ mole fraction in [MPI][BF_4] and $LiBF_4$ mixtures for $0 < x_{\mathrm{LiBF_4}} < 0.25$. For consistency of self-diffusion coefficient determination, the hydrogen adjacent to the two nitrogen atoms in imidazolium was selected in this study. Fig. 7 shows the temperature dependence of the self-diffusion coefficients of the

cation and anion species (D_{MPI^+} , D_{Li^+} , and $D_{BF_4^-}$), and the summation of the cation and anion (D_{total} = $x D_{Li^+} + (1-x) D_{MPI^+} + D_{BF_4^-}$) for these binary IL solutions, the experimental self-diffusion coefficients D (cm^2 s^{-1}) and activation energy $E_{a,D}$ (kJ/mol) for $LiBF_4$-doped [MPI][BF_4] and neat [MPI][BF_4] are summarized in Table 7. As shown in Fig. 7, some of the temperature dependence curves of D_{MPI^+} , D_{Li^+} , $D_{BF_4^-}$ and D_{total} cannot be expressed by a simple linear function. However, the Vogel–Tamman–Fulcher (VTF) equation fits the experimental data very well over the entire temperature range.

$$D = D_o \exp[\frac{-B'}{(T - T_o)}] \qquad (10)$$

where the constants D_o (cm^2 s^{-1}), B' (K), and T_o (K) are adjustable parameters. The best-fit parameters of the ionic diffusivity are summarized in Table 8 and Table 9. As shown in Fig. 7, the sum of the cationic and anionic diffusion coefficients (D_{total}) for the neat [MPI][BF_4] and $LiBF_4$-doped [MPI][BF_4] follows the order: (x_{LiBF_4} = 0) > (x_{LiBF_4} = 0.0672) > (x_{LiBF_4} = 0.1111) > (x_{LiBF_4} = 0.1543) > (x_{LiBF_4} = 0.2054) > (x_{LiBF_4} = 0.2503).

Ionic transference numbers at 303 K are shown in Table 7 to compare the self-diffusion coefficients of each ion, the ionic transference number t_i [53] is defined as:

$$t_i = \frac{x_i D_i}{\Sigma x_i D_i} \qquad (11)$$

The ionic transference number of the MPI^+ is comparable to that of BF_4^- in neat [MPI][BF_4] at all temperatures. However, the ionic transference numbers of the MPI^+ and Li^+ increase and the BF_4^- decrease with increasing $LiBF_4$ mole fraction in [MPI][BF_4] and $LiBF_4$ mixtures. The ionic transference numbers of ions in ILs can be ascribed to influence by the shape of the ions and the local interaction between the cations and anions [54].

3.3. Molar conductivity evaluated from the PGSE-NMR diffusion coefficients

The Nernst-Einstein equation is applied to calculate molar conductivity (Λ_{NMR}) from the PGSE-NMR diffusion coefficients:

$$\Lambda_{NMR} = \frac{Ne^2 (x_{MPI^+} D_{MPI^+} + D_{BF_4^-} + x_{Li^+} D_{Li^+})}{kT} \qquad (12)$$

where N is the Avogadro number, e is the electric charge on each ionic carrier ($1.602*10^{-19}$ Coulomb), x_{MPI^+} and x_{Li^+} are the molar ratio of IL and $LiBF_4$, respectively, k is the Boltzmann constant ($1.38*10^{-23}$), and T is the absolute temperature (K). The temperature dependence of the molar

conductivity calculated from the ionic diffusion coefficient and Eq. 12 is shown in Fig. 8 and the best-fit parameters of the VTF equation are listed in Table 4. The experimental molar conductivity value (Λ) is lower than that of the calculated molar conductivity (Λ_{NMR}) over the entire temperature range, which has been established as one of the important phenomena associated with ionic liquids [55].

Table 7. Experimental self-diffusion coefficients D ($cm^2\ s^{-1}$), ion transference number t at 303 K, and activation energy $E_{a,D}$ (kJ/mol) for $LiBF_4$-doped [MPI][BF_4] and neat [MPI][BF_4]. Transference number t_i is defined as: $t_i = x_iD_i/\Sigma x_iD_i$.

	ion	D / $cm^2\ s^{-1}$	t	$E_{a,D}$ / kJ $mole^{-1}$
neat [MPI][BF_4]	MPI^+	1.45×10^{-7}	0.509	33.66
	BF_4^-	1.40×10^{-7}	0.491	33.99
x_{LiBF_4} = 0.0672	MPI^+	1.08×10^{-7}	0.513	35.04
	Li^+	9.76×10^{-9}	0.0033	36.11
	BF_4^-	9.50×10^{-8}	0.484	36.40
x_{LiBF_4} = 0.1111	MPI^+	8.68×10^{-8}	0.531	36.21
	Li^+	7.24×10^{-9}	0.0055	37.19
	BF_4^-	6.72×10^{-8}	0.463	38.33
x_{LiBF_4} = 0.1543	MPI^+	7.86×10^{-8}	0.527	37.56
	Li^+	6.61×10^{-9}	0.0081	38.31
	BF_4^-	5.87×10^{-8}	0.465	38.88
x_{LiBF_4} = 0.2054	MPI^+	6.05×10^{-8}	0.540	38.82
	Li^+	4.62×10^{-9}	0.0107	39.60
	BF_4^-	4.00×10^{-8}	0.449	41.25
x_{LiBF_4} = 0.2503	MPI^+	4.81×10^{-8}	0.543	40.39
	Li^+	3.28×10^{-9}	0.0124	42.42
	BF_4^-	2.95×10^{-8}	0.445	42.57

Table 8. VTF equation parameters of self-diffusion coefficient data ($D = D_o \exp[-B'/(T - T_o)]$) from the MPI^+ of [MPI][BF_4] and BF_4^- of $LiBF_4$ and [MPI][BF_4].

Molar fraction of $LiBF_4$	D_{MPI}^+				D_{BF4}^-			
	D_o/$cm^2\ s^{-1}$	T_o (K)	B' (K)	R^{2a}	D_o/$cm^2\ s^{-1}$	T_o (K)	B' (K)	R^{2a}
neat [MPI][BF_4]	5.15×10^{-5}	198.3	614.8	0.999	7.86×10^{-5}	188.8	722.9	0.999
x_{LiBF_4} = 0.0672	5.48×10^{-5}	196.4	663.6	0.999	8.47×10^{-5}	187.5	784.3	0.999
x_{LiBF_4} = 0.1111	6.72×10^{-5}	189.2	757.0	0.999	1.26×10^{-4}	180.3	924.5	0.999
x_{LiBF_4} = 0.1543	8.01×10^{-5}	188.4	795.2	0.999	5.51×10^{-5}	197.9	719.4	0.999
x_{LiBF_4} = 0.2054	8.50×10^{-5}	188.1	832.6	0.999	1.04×10^{-4}	184.8	929.9	0.999
x_{LiBF_4} = 0.2503	8.19×10^{-5}	190.1	839.8	0.999	9.85×10^{-5}	181.3	988.3	0.999

[a] Correlation coefficient.

Table 9. VTF equation parameters of self-diffusion coefficient data ($D = D_o \exp[-B'/(T - T_o)]$) from Li^+ of $LiBF_4$ and ($MPI^+ + BF_4^- + Li^+$) of ($LiBF_4$ and [MPI][BF_4]).

Molar fraction of $LiBF_4$	D_{Li}^+				D_{total}			
	D_o/cm^2 s^{-1}	T_o (K)	B' (K)	R^{2a}	D_o/cm^2 s^{-1}	T_o (K)	B' (K)	R^{2a}
neat [MPI][BF_4]	---	---	---	---	1.26×10^{-4}	193.8	664.9	0.999
x_{LiBF_4} = 0.0672	9.51×10^{-6}	184.3	816.8	0.999	1.32×10^{-4}	191.9	722.7	0.999
x_{LiBF_4} = 0.1111	1.06×10^{-5}	179.1	903.6	0.999	2.17×10^{-4}	179.8	900.6	0.999
x_{LiBF_4} = 0.1543	1.05×10^{-5}	182.0	891.4	0.999	2.00×10^{-4}	183.4	881.7	0.999
x_{LiBF_4} = 0.2054	4.43×10^{-6}	199.1	712.8	0.999	1.60×10^{-4}	187.4	866.1	0.999
x_{LiBF_4} = 0.2503	9.89×10^{-6}	184.5	949.7	0.999	1.86×10^{-4}	182.6	955.9	0.999

[a] Correlation coefficient.

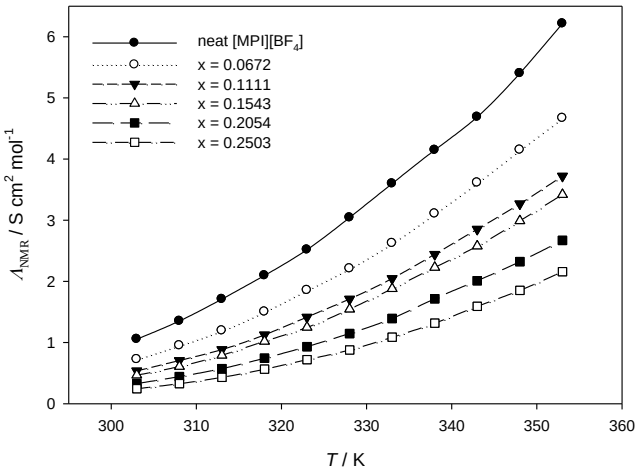

Figure 8. Dependence of molar conductivity (Λ_{NMR}) on temperature for neat [MPI][BF_4] and $LiBF_4$-doped [MPI][BF_4]. Λ_{NMR} is calculated from PGSE-NMR diffusion coefficient and Nernst-Einstein equation.

3.4. Comparison of the dynamic properties depending on temperature

Fig. 9 shows the activation energies of the reciprocal of viscosity, the ionic conductivity, and individual ion diffusion against the $LiBF_4$ concentration. The activation energies for the reciprocal of viscosity are larger than those of the ionic conductivity and molar conductivity, however, they are smaller than those of individual ion diffusion at $0 < x_{LiBF_4} < 0.25$. The activation energy of the ionic conductivity is comparable to molar conductivity and shows a minimum at a mole fraction of $LiBF_4$ near x = 0.0672, however, the activation energy of the reciprocal of viscosity and individual ion diffusion showed an increased tendency with increasing $LiBF_4$ concentration. The activation energy of individual ion diffusion with the $LiBF_4$ concentration is in the order: $D_{BF_4^-} > D_{Li^+} > D_{MPI^+}$. The

increase of the activation energy of the individual ion diffusion with $LiBF_4$ concentration indicates a reduction of the translational motions due to the higher viscosity in the concentrated samples. The different tendency between the activation energy of the ionic conductivity and individual ion diffusion with $LiBF_4$ concentration can be attributed to different types between ionic conductivity and individual ion diffusion. Ion diffusion coefficients are measured by PGSE-NMR and consider the isolated, paired, and clustered ions including noncharge neutral ion clusters, but the ionic conductivity is affected by ion transfer velocity and the number of "electrochemically" active ions.

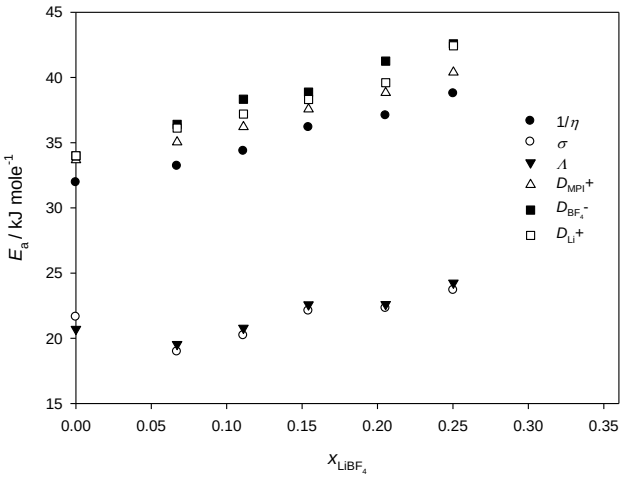

Figure 9. Dependencies of the activation energies of the individual ion diffusion, ionic conductivity, and (reciprocal of the) viscosity in neat [MPI][BF_4] and $LiBF_4$-doped [MPI][BF_4].

4. CONCLUSIONS

We have studied electrical transport and diffusion processes in [MPI][BF_4]/$LiBF_4$ mixtures with different mole fraction of $LiBF_4$. The density and viscosity in the ILs increased with increasing concentration of $LiBF_4$, whereas the conductivity, molar conductivity, and self-diffusion coefficient of each ionic species decreased with increasing concentration of $LiBF_4$. The molar conductivities were compared for the values obtained by the electrochemical conductivity (Λ) and the values calculated from the pulsed-gradient spin-echo nuclear magnetic resonance method (diffusive conductivity) (Λ_{NMR}). The Λ/Λ_{NMR} values for the $LiBF_4$-doped [MPI][BF_4] studied are less than unity, indicating that not all the diffusive species contribute to the ionic conduction (i.e. free-ions, ionic pair or/and cluster coexist in $LiBF_4$-doped [MPI][BF_4]). The different tendency between the activation energy of the Λ and Λ_{NMR} with $LiBF_4$ concentration can be attributed to Λ_{NMR} is calculated by PGSE-NMR and consider the isolated, paired, and clustered ions including noncharge neutral ion clusters, however, the Λ is affected by ion transfer velocity and the number of "electrochemically" active ions.

ACKNOWLEDGEMENTS
The authors would like to thank the National Science Council of the Republic of China for financially supporting this project.

References

1. H. Ohno, Electrochemical Aspects of Ionic Liquids, Wiley, New Jersey, 2005.
2. P. Wasserscheid, W. Keim, *Angew. Chem. Int. Ed.*, 39 (2000) 3772.
3. T.Y. Wu, S.G. Su, K.F. Lin, Y.C. Lin, H.P. Wang, M.W. Lin, S.T. Gung, I.W. Sun, *Electrochim. Acta*, 56 (2011) 7278.
4. E. Abitelli, S. Ferrari, E. Quartarone, P. Mustarelli, A. Magistris, M. Fagnoni, A. Albini, C. Gerbaldi, *Electrochim. Acta*, 55 (2010) 5478.
5. T.Y. Wu, B.K. Chen, L. Hao, Y.C. Lin, H.P. Wang, C.W. Kuo, I.W. Sun, *Int. J. Mol. Sci.*, 12 (2011) 8750.
6. T. Kakibe, N. Yoshimoto, M. Egashira, M. Morita, *Electrochem. Commun.*, 12 (2010) 1630.
7. T.Y. Wu, S.G. Su, H.P. Wang, I.W. Sun, *Electrochem. Commun.*, 13 (2011) 237.
8. Z.H. Li, Q.L. Xia, L.L. Liu, G.T. Lei, Q.Z. Xiao, D.S. Gao, X.D. Zhou, *Electrochim. Acta*, 56 (2010) 804.
9. Y.X. An, P.J. Zuo, X.Q. Cheng, L.X. Liao, G.P. Yin, *Int. J. Electrochem. Sci.*, 6 (2011) 2398.
10. H.B. Han, K. Liu, S.W. Feng, S.S. Zhou, W.F. Feng, J. Nie, H. Li, X.J. Huang, H. Matsumoto, M. Armand, Z.B. Zhou, *Electrochim. Acta*, 55 (2010) 7134.
11. X.G. Sun, S. Dai, *Electrochim. Acta*, 55 (2010) 4618.
12. M.R. Ganjali, H. Ganjali, M. Hosseini, P. Norouzi, *Int. J. Electrochem. Sci.*, 5 (2010) 967.
13. M.R. Ganjali, S. Aghabalazadeh, M. Rezapour, M. Hosseini, P. Norouzi, *Int. J. Electrochem. Sci.*, 5 (2010) 1743.
14. M. Pandurangachar, B.E.K. Swamy, B.N. Chandrashekar, O. Gilbert, S. Reddy, B.S. Sherigara, *Int. J. Electrochem. Sci.*, 5 (2010) 1187.
15. P. Norouzi, Z. Rafiei-Sarmazdeh, F. Faridbod, M. Adibi, M.R. Ganjali, *Int. J. Electrochem. Sci.*, 5 (2010) 367.
16. F. Faridbod, M.R. Ganjali, M. Pirali-Hamedani, P. Norouzi, *Int. J. Electrochem. Sci.*, 5 (2010) 1103.
17. M.R. Ganjali, M.H. Eshraghi, S. Ghadimi, S.M. Moosavi, M. Hosseini, H. Haji-Hashemi, P. Norouzi, *Int. J. Electrochem. Sci.*, 6 (2011) 739.
18. M.R. Ganjali, T. Poursaberi, M. Khoobi, A. Shafiee, M. Adibi, M. Pirali-Hamedani, P. Norouzi, *Int. J. Electrochem. Sci.*, 6 (2011) 717.
19. P. Norouzi, M. Hosseini, M.R. Ganjali, M. Rezapour, M. Adibi, *Int. J. Electrochem. Sci.*, 6 (2011) 2012.
20. M.R. Ganjali, M.R. Moghaddam, M. Hosseini, P. Norouzi, *Int. J. Electrochem. Sci.*, 6 (2011) 1981.
21. M.R. Ganjali, M. Hosseini, M. Pirali-Hamedani, H.A. Zamani, *Int. J. Electrochem. Sci.*, 6 (2011) 2808.
22. M.R. Ganjali, M. Rezapour, S.K. Torkestani, H. Rashedi, P. Norouzi, *Int. J. Electrochem. Sci.*, 6 (2011) 2323.
23. T.H. Tsai, K.C. Lin, S.M. Chen, *Int. J. Electrochem. Sci.*, 6 (2011) 2672.
24. T.Y. Wu, M.H. Tsao, F.L. Chen, S.G. Su, C.W. Chang, H.P. Wang, Y.C. Lin, W.C. Ou-Yang, I.W. Sun, *Int. J. Mol. Sci.*, 11 (2010) 329.
25. S.Y. Ku, S.Y. Lu, *Int. J. Electrochem. Sci.*, 6 (2011) 5219.
26. T.Y. Wu, M.H. Tsao, F.L. Chen, S.G. Su, C.W. Chang, H.P. Wang, Y.C. Lin, I.W. Sun, *J. Iran. Chem. Soc.*, 7 (2010) 707.

27. M.H. Tsao, T.Y. Wu, H.P. Wang, I.W. Sun, S.G. Su, Y.C. Lin, C.W. Chang, *Mater. Lett.*, 65 (2011) 583.
28. T.Y. Wu, M.H. Tsao, S.G. Su, H.P. Wang, Y.C. Lin, F.L. Chen, C.W. Chang, I.W. Sun, *J. Braz. Chem. Soc.*, 22 (2011) 780.
29. Q. Che, R. He, J. Yang, L. Feng, R.F. Savinell, *Electrochem. Commun.*, 12 (2010) 647.
30. G. Lakshminarayana, M. Nogami, *Electrochim. Acta*, 55 (2010) 1160.
31. J. Gao, J. Liu, W. Liu, B. Li, Y. Xin, Y. Yin, Z. Zou, *Int. J. Electrochem. Sci.*, 6 (2011) 6115.
32. P.N. Tshibangu, S.N. Ndwandwe, E.D. Dikio, *Int. J. Electrochem. Sci.*, 6 (2011) 2201.
33. K.K. Denshchikov, M.Y. Izmaylova, A.Z. Zhuk, Y.S. Vygodskii, V.T. Novikov, A.F. Gerasimov, *Electrochim. Acta*, 55 (2010) 7506.
34. T.Y. Wu, S.G. Su, Y.C. Lin, H.P. Wang, M.W. Lin, S.T. Gung, I.W. Sun, *Electrochim. Acta*, 56 (2010) 853.
35. A.N. Soriano, B.T. Doma, M.H. Li, *J. Taiwan Inst. Chem. Eng.*, 41 (2010) 115.
36. T.Y. Wu, S.G. Su, S.T. Gung, M.W. Lin, Y.C. Lin, C.A. Lai, I.W. Sun, *Electrochim. Acta*, 55 (2010) 4475.
37. K. Liu, Y.X. Zhou, H.B. Han, S.S. Zhou, W.F. Feng, J. Nie, H. Li, X.J. Huang, M. Armand, Z.B. Zhou, *Electrochim. Acta*, 55 (2010) 7145.
38. T.Y. Wu, B.K. Chen, L. Hao, Y.C. Peng, I.W. Sun, *Int. J. Mol. Sci.*, 12 (2011) 2598.
39. T.Y. Wu, I.W. Sun, S.T. Gung, B.K. Chen, H.P. Wang, S.G. Su, *J. Taiwan Inst. Chem. Eng.*, 42 (2011) 874.
40. Y. Litaeim, M. Dhahbi, *J. Mol. Liq.*, 155 (2010) 42.
41. T.Y. Wu, S.G. Su, S.T. Gung, M.W. Lin, Y.C. Lin, W.C. Ou-Yang, I.W. Sun, C.A. Lai, *J. Iran. Chem. Soc.*, 8 (2011) 149.
42. T.Y. Wu, H.C. Wang, S.G. Su, S.T. Gung, M.W. Lin, C.B. Lin, *J. Chin. Chem. Soc.*, 57 (2010) 44.
43. K. Yoshida, M. Tsuchiya, N. Tachikawa, K. Dokko, M. Watanabe, *J. Phys. Chem. C*, 115 (2011) 18384.
44. T.Y. Wu, S.G. Su, H.P. Wang, Y.C. Lin, S.T. Gung, M.W. Lin, I.W. Sun, *Electrochim. Acta*, 56 (2011) 3209.
45. X. Zhang, C.-G. Li, C.-H. Ye, M.-L. Liu, *Anal. Chem.*, 153 (2001) 48.
46. T.Y. Wu, H.C. Wang, S.G. Su, S.T. Gung, M.W. Lin, C.B. Lin, *J. Taiwan Inst. Chem. Eng.*, 41 (2010) 315.
47. J.E. Tanner, E.O. Stejskal, *J. Chem. Phys.*, 49 (1968) 1768.
48. K.R. Seddon, A.S. Starck, M.J. Torres, ACS Symposium Series 901, Washington, DC, 2004.
49. H. Every, A.G. Bishop, M. Forsyth, D.R. MacFarlane, *Electrochim. Acta*, 45 (2000) 1279.
50. T.Y. Wu, B.K. Chen, L. Hao, K.F. Lin, I.W. Sun, *J. Taiwan Inst. Chem. Eng.*, 42 (2011) 914.
51. M. Yoshizawa, W. Xu, C.A. Angell, *J. Am. Chem. Soc.*, 125 (2003) 15411.
52. T.Y. Wu, I.W. Sun, M.W. Lin, B.K. Chen, C.W. Kuo, H.P. Wang, Y.Y. Chen, S.G. Su, *J. Taiwan Inst. Chem. Eng.*, 43 (2012) 58.
53. F. Castiglione, E. Ragg, A. Mele, G.B. Appectecchi, M. Montanino, S. Passerini, *J. Phys. Chem. Lett.*, 2 (2011) 153.
54. T.Y. Wu, I.W. Sun, S.T. Gung, M.W. Lin, B.K. Chen, H.P. Wang, S.G. Su, *J. Taiwan Inst. Chem. Eng.*, 42 (2011) 513.
55. H. Tokuda, K. Hayamizu, K. Ishii, M.A.B.H. Susan, M. Watanabe, *J. Phys. Chem. B*, 109 (2005) 6103.

© 2012 by ESG (www.electrochemsci.org)